SIMULTANEOUS DUAL-WAVELENGTH GENERATION FROM VERTICAL EXTERNAL-CAVITY SURFACE-EMITTING SEMICONDUCTOR LASERS

S. Ranta [a], T. Leinonen [a], A. Härkönen [a], A. Laakso [a], Y. Morozov [b], and M. Pessa [a]

[a] *Optoelectronics Research Centre, Tampere University of Technology, P.O. Box 692, FI-33101 Tampere, Finland*
E-mail: sanna.ranta@tut.fi
[b] *Institute of Radio Engineering and Electronics (Saratov Branch), Russian Academy of Sciences, Zelenaya 38, 410019 Saratov, Russia*

We demonstrate dual-wavelength emission from optically pumped vertical-external-cavity surface-emitting lasers (VECSELs) with two different gain mirror designs. The first gain mirror design ($S1$) generated an optical output power of 0.39 W at $\lambda_S = 984$ nm and 0.30 W at $\lambda_L = 1042$ nm. A VECSEL using the second gain mirror design ($S2$) generated a maximum optical output power of 0.75 W at $\lambda_S = 966$ nm and 1.38 W at $\lambda_L = 1047$ nm. VESCELs using either gain mirror design exhibited self-pulsating behaviour in the high output power regime. In the VECSEL using the $S1$ gain mirror design, self-pulsation started beyond the λ_S output power of 140 mW and λ_L output power of 115 mW. The corresponding output power limits in the VECSEL using the $S2$ gain mirror were 300 mW for both wavelengths.

Keywords: vertical external-cavity surface-emitting lasers, resonant periodic gain structure, semiconductor lasers

PACS: 42.55.Px, 42.60.By

1. Introduction

Two-wavelength lasers are particularly interesting light sources with applications ranging from nonlinear frequency mixing [1] to two-wavelength interferometry [2]. An ideal light source for these applications would emit two diffraction-limited, high power co-axial beams with sufficiently large wavelength separation. Due to their compact size, large gain bandwidth, and possibility for wavelength tailoring, semiconductor lasers are particularly well suited for two-wavelength applications.

A vertical coupled-cavity surface-emitting laser is capable of meeting these requirements [3]. Furthermore, such laser geometry offers good beam quality in a compact form. Coupled-cavity structures, however, can only achieve relatively small wavelength separation, typically less than 30 nm in the near infrared, with fairly small output powers in the order of milliwatts [3]. This separation is not enough for some applications. For example, the wavelength separation is not large enough to reach difference frequencies in the mid-infrared region. Another device capable of dual-wavelength emission is a wide-band-gain semiconductor optical amplifier (SOA) using an external grating to couple two different gain stripes, located on a single chip, into a single cavity [4]. With this approach, dual-wavelength emission with a wavelength separation of more than 170 nm in the near infrared can be achieved [5]. An arbitrarily large wavelength separation can be achieved from a similar device, a grating-coupled edge-emitting laser, which comprises two or more chips emitting light at different wavelengths and an external grating that combines the two beams into one co-axial beam. These approaches have disadvantages in terms of the complex optics required for coupling the elliptical beams emitted by the gain stripes.

To combine the advantageous features of vertical coupled-cavity devices and those offered by broadband SOAs we have developed optically pumped vertical-external-cavity surface-emitting lasers (VECSELs [6, 7]) with emission at two wavelengths which are well separated. Figure 1 shows typical VECSEL elements. The laser cavity is formed between the gain mirror and an external mirror, which also acts as an output coupler. The gain mirror has a resonant periodic gain (RPG) structure comprising quantum wells (QWs) for gain and a distributed Bragg reflector [8]. The pump light is ab-
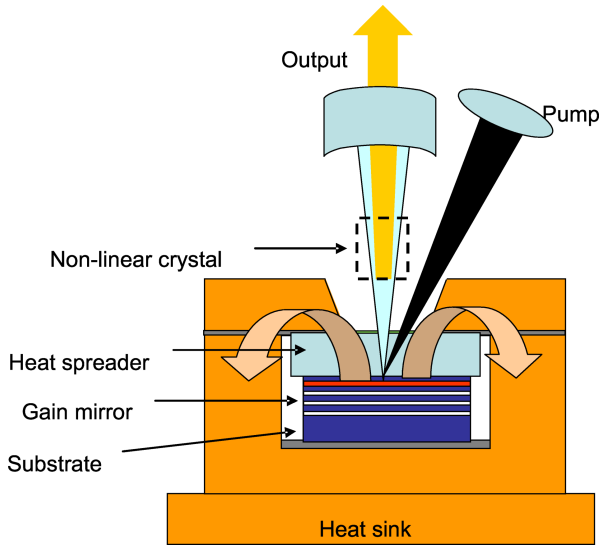
Fig. 1. Schematic of a typical VECSEL set-up.

Fig. 2. Refractive index profile of $S1$ in resonant periodic gain region and optical field intensities at λ_S (dashed line) and λ_L (solid line). Diamond/semiconductor interface is located at 0 optical path length. Pump light enters $S1$ from the left side of this interface.

Fig. 3. Spectra of samples with (solid line) and without (dashed line) carrier blocking layers (CBLs).

sorbed by the quantum well barriers and the carriers are captured by the QWs. Efficient heat conduction away from the gain mirror is crucial for high-power operation. Typically, diamond [9] is used as a heat spreader which is located either inside the laser cavity (as in the figure) [10] or outside the laser cavity (see, for example, [7]).

The VECSELs are designed to emit the two light beams co-axially sharing a single external cavity, which makes these devices compact. The vertical external-cavity geometry offers scalability to watt-level optical output power in a circular TEM_{00} mode. Furthermore, VECSEL development requires relatively simple processes, and the external cavity enables intra-cavity optical components, such as nonlinear optical crystals, semiconductor saturable absorbers, and wavelength selective filters to be incorporated. The possibility to exploit intra-cavity frequency conversion and wavelength filtering is particularly important because it enables efficient nonlinear conversion and high-power single-frequency operation [11].

2. Design of the gain structures

There are two major obstacles involved in the design of a gain mirror for a semiconductor based dual-wavelength VECSEL. The first, and the more difficult to deal with, is the absorption of the short wavelength signal, λ_S, in the long wavelength, λ_L, quantum-well gain medium. The absorption is caused by the states above the lasing wavelength. The second problem is the equalization of the beam intensities. The need for equalization arises from non-uniform pumping of the
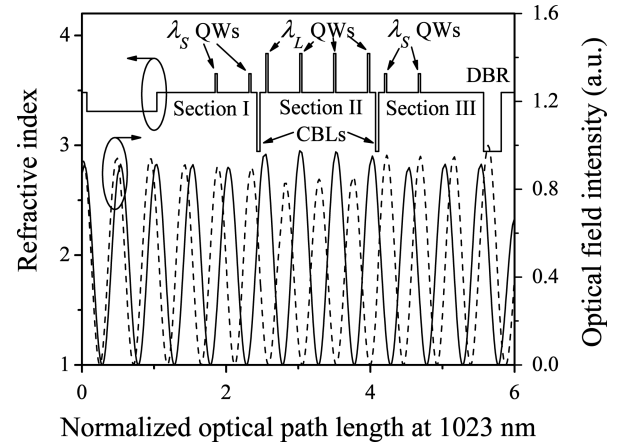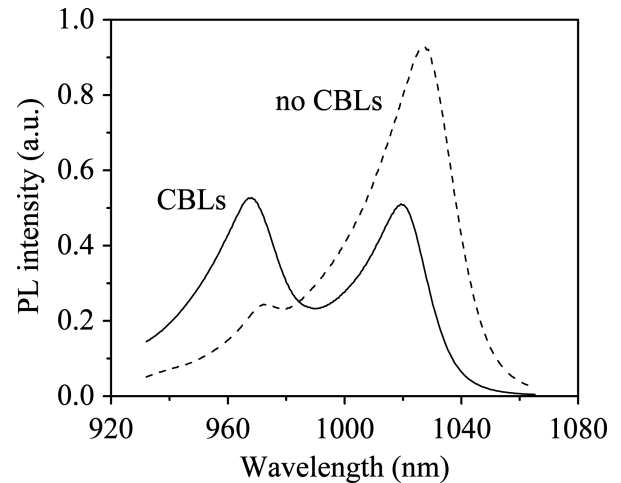
quantum wells inside a VECSEL structure – the pump light is absorbed as it traverses the gain mirror, being about 20% of the initial value close to the bottom of the resonant period gain structure used in VECSELs.

The gain mirrors we have designed for emissions at two wavelengths (λ_S & λ_L) are based on QWs. The first structure ($S1$) had QWs inside a single RPG structure [12]. The single RPG, however, was divided into three sections by carrier blocking layers (CBLs, Fig. 2). The first and third sections contained two λ_S QWs each and the second four λ_L QWs. The blocking layers eliminated carrier flow between the three sections, allowing different carrier populations for each section. Had the sections, and thus the QWs, shared the same carrier population, the λ_S QWs would not have been inverted at all. This is because most of the pump-generated carriers would have been captured by the deeper λ_L QWs
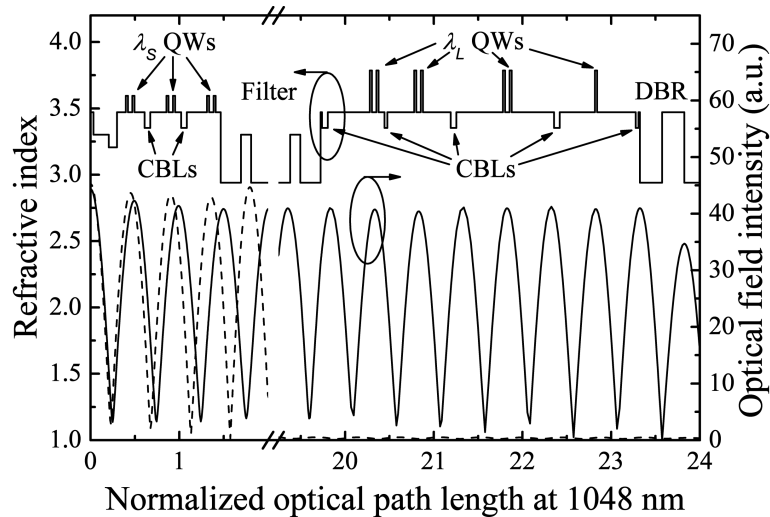
Fig. 4. Refractive index profile of $S2$ in both resonant periodic gain regions and optical field intensities at λ_S (dashed line) and λ_L (solid line). Optical pumping is introduced and laser emission occurs at the same directions as in $S1$ (see Fig. 1).

at the expense of the shallower λ_S QWs, leading to an unequal pumping of the different QW types. This pumping inequality was tested with two samples, one of which had one λ_L and one λ_S QWs in the same section, whereas the other had a carrier blocking layer between the QWs (see Fig. 3). The sample without the CBLs showed much worse photoluminescence performance at the shorter wavelength, as seen in Fig. 3. Furthermore, the inequality of the pump beam intensity had to be taken into account in the VECSEL design. The beam intensity drops as it is absorbed by the RPG structure. This leads to highest pumping of the QWs near the surface. This phenomenon is enhanced by the CBLs as compared to the conventional VECSEL mirrors without such blocking layers. The pumping inequality caused by the pump beam intensity decrease was compensated for by having two of the λ_S QWs in the high intensity pumping regime (section *I* in Fig. 2) and two in the low intensity pumping regime (section *III*), whereas all four λ_L QWs were located in the intermediate intensity pumping regime (section *II*).

A highly reflective distributed Bragg reflector (DBR) made of AlAs/GaAs was situated beneath the RPG to provide the mirror feedback for the laser cavity. The index contrast of such a mirror is just sufficient to realize a stop band wide enough for both wavelengths. The material dispersion of the gain mirror alone would not have been enough to separate the two wavelengths far enough to have λ_L anti-nodes and λ_S nodes coincide in the RPG structure at the λ_L QW locations. The required separation was provided by the different phase-shifts experienced by the two wavelengths near the opposite edges of the DBR.

The second gain mirror structure ($S2$) was developed to reduce the stringent growth precision required by $S1$, in which a small misalignment of the λ_S standing optical wave in respect to the λ_L QWs (about 6 nm) is enough to cause significant absorption of λ_S [13]. Furthermore, the design allowed a more straightforward implementation of larger wavelength separations than $S1$. A large wavelength separation is also possible with a single-RPG structure similar to $S1$, but the DBR has to be replaced with one having multiple stop bands.

The $S2$ had two separate RPG structures, one for each wavelength [14]. The RPG containing the λ_S QWs was closer to the gain mirror surface (see Fig. 4). The QWs were organized in sections, each containing a single QW pair, except for the last λ_L QW. All sections were separated by either CBLs or a long-wave pass filter. Since the pump beam intensity had dropped significantly from the initial value (to about 23%) at the last section, the section had only one QW. The pumping of the sections was equalized by having each section absorb similar amounts of the pump light. This was done by tuning the barrier layer thicknesses of each section. The amount of pump light absorbed was deduced by simulating the field intensity within the gain mirror structure, taking into account the absorption in the QW and barrier layers.

The λ_L QWs were made of 7-nm $Ga_{0.75}In_{0.25}As$ layers and the λ_S QWs were made of 7-nm $Ga_{0.86}In_{0.14}As$ layers, resulting in lattice strains of -1.79 and -1.00%, respectively. The CBL material was $GaAs_{0.70}P_{0.30}$, whose tensile lattice strain (1.08%)
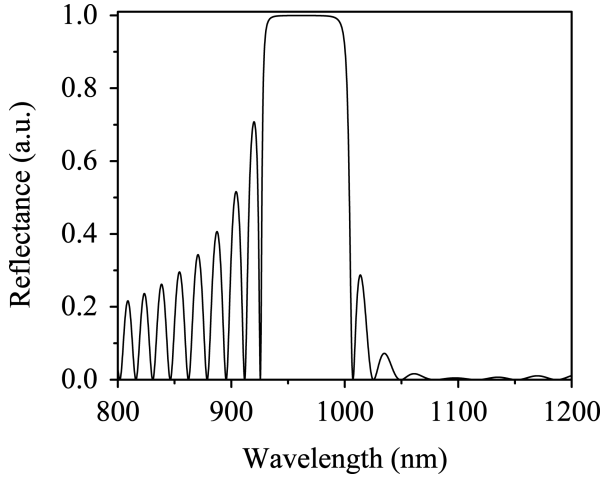
Fig. 5. Reflectance spectrum of the long-wave pass filter. The filter is designed to reflect λ_S and transmit λ_L. Therefore, λ_S is located in the stop band of the filter and λ_L in the minimum reflectance region.

Table 1. Semiconductor layer structure of the PL sample.

Layer	Material	Thickness (nm)
Cap	GaAs	25
Carrier confinement	AlAs	100
Barrier	GaAs	100
λ_S QW	$Ga_{0.86}In_{0.14}As$	7
Barrier	GaAs	25
CBL	AlAs	15
Barrier	GaAs	25
λ_L QW	$Ga_{0.75}In_{0.25}As$	7
Barrier	GaAs	100
Carrier confinement	AlAs	300
Buffer	GaAs	200
Substrate	n-GaAs	

was designed to compensate fully the lattice strain induced by the QWs according to

$$\varepsilon_{QW,\lambda_i}\, N_{QW,\lambda_i}\, d_{QW,\lambda_i} = \varepsilon_{CBL,\lambda_i}\, N_{CBL,\lambda_i}\, d_{CBL,\lambda_i}\,. \tag{1}$$

In Eq. (1) N_{QW,λ_i} and N_{CBL,λ_i} are the total number of λ_i QWs and CBLs that are located in λ_i RPG, d_{QW,λ_i} and d_{CBL,λ_i} are their thicknesses, and $\varepsilon_{QW,\lambda_i}$ and $\varepsilon_{CBL,\lambda_i}$ are their lattice strains.

The RPGs in $S2$ were separated by a long-wave pass filter, which was designed to have a transmission maximum for λ_L and a reflectance maximum for λ_S, thus keeping λ_S from entering the λ_L QWs and preventing absorption. The filter had a low amount of undulating reflection on the pass-side, which diminished as the wavelength increased (see Fig. 5). Since λ_L was relatively close to the cut-off wavelength of the filter, the filter still had a small amount of reflectivity close to λ_L and was fitted in such a way that λ_L coincided with a minimum of the undulating reflection (see Fig. 5). The filter had 39 periods of $Al_{0.30}Ga_{0.7}As/AlAs/Al_{0.30}Ga_{0.7}As$, surrounded by AlAs phase-matching layers to reduce the ripple amplitude on the pass-band side. The thickness of the AlAs layers was 81.41 nm and the thickness of the $Al_{0.30}Ga_{0.7}As$ layers was about 36 nm. The mirror feedback for the λ_S was provided by the filter, and the feedback for the λ_L by a DBR beneath the λ_L RPG structure. Due to the thick filter (about 6 μm), $S2$ had a significantly higher thermal impedance for λ_L as compared to $S1$.

Both structures were terminated by a thin GaAs capping layer (thickness $d = 20$ nm in $S1$ and $d = 10$ nm in $S2$), whose purpose was to protect the $Al_{0.30}Ga_{0.7}As$

layer during the processing steps involved in the chip mounting. Beneath the capping layer both structures had a window layer ($d = 300$ nm in $S1$ and $d = 55$ nm in $S2$) to prevent carriers leaking to the gain mirror surface. The thicknesses of the capping and the window layers were made as thin as possible in order to minimize the thermal impedance between the gain regions and the gain mirror surface. The structures were resonant for both λ_S and λ_L. In $S1$, the window layer had to be thicker than in $S2$ in order for both λ_S and λ_L to be resonant at the same time. In $S2$, the λ_S resonance was first matched with the window layer, and the λ_L resonance was then matched with the thicknesses of the λ_L gain section barrier layers. In both designs, λ_L QWs and λ_S QWs are located near the antinodes of the optical standing field of the corresponding wavelength in order to maximize the gain for each wavelength.

3. Gain mirror fabrication and characterization set-ups

Both $S1$ and $S2$ were grown and attached to gain-mirror carriers in similar fashions. The gain mirrors were fabricated in a single solid-source molecular-beam-epitaxy growth step on a 2″ n-GaAs substrate. For the laser to operate at the desired wavelength, the room-temperature QW emission wavelength was calibrated before the gain mirror growth by using a photoluminescence (PL) sample containing QWs for both wavelengths, CBL between the QWs, and carrier confining AlAs-layers (see Table 1). A thin GaAs layer was grown on top of the photoluminescence sample in order to prevent the AlAs layers from oxidation. To accommodate the wavelength shift induced by heating of the gain mirrors during laser operation, the room temperature emission targets were set about 15 nm shorter than the desired lasing wavelengths. The emission wave-
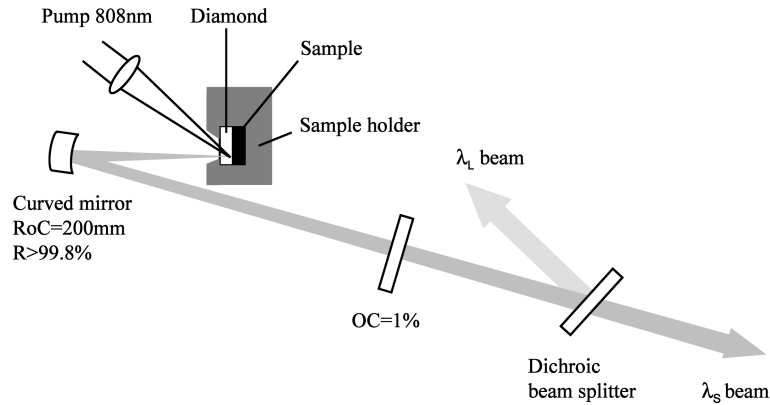
Fig. 6. VECSEL configuration. The distance between the curved mirror and the gain chip is 130 mm for $S1$ and 135 mm for $S2$. The planar output coupler (OC) is located 385 and 241 mm away from the curved mirror in the case of $S1$ and $S2$, respectively.

length was tuned by changing the QW compositions according to measurement data obtained from the PL sample. Since accurate layer thicknesses are crucial for proper device operation, the growth rates of aluminium and gallium cells were calibrated carefully before each gain mirror growth.

High arsenic beam flux, as determined by the chamber background pressure, was employed during the epitaxial growth ($p \sim 1.3$–$1.4 \cdot 10^{-6}$ mbar), since this seemed to yield better crystalline quality as compared to the pressure typically used, for example, during the growth of edge-emitting lasers ($p \sim 3$–$4 \cdot 10^{-7}$ mbar). For surface emitting lasers, a pressure of $p \sim 6 \cdot 10^{-7}$ mbar would usually yield a rough wafer surface, as determined by examining the surface with a phase-contrast microscope. The surface roughness problem was particularly severe for $S2$. This problem is most likely linked to the GaAs/AlAs interfaces present in the DBR and filter layers. $S2$ contains more of these interfaces ($S1$: 62 interfaces, $S2$: 143 interfaces). During the DBR and filter structure growth in $S2$, the growth was interrupted for 5 seconds at each DBR or filter interface. It was believed that this approach would help smooth wafer surfaces to be achieved. This technique, however, did not result in a noticeable improvement.

After the epitaxial growth, the wafers were diced into chips of about 2×2 mm^2 in size. The chips were capillary bonded [15] on a 300-μm thick transparent type IIa diamond window which functioned as an intra cavity heat spreader. The diamond window was attached to a copper sample holder by mechanical pressure and with the aid of thin (50 μm) indium foil. The heat generated at the gain mirror would exit through the diamond heat spreader and the indium foil to the copper mount. After the chip bonding, a two-layer anti-reflective dielectric

coating was applied to the diamond surface by electron beam evaporation.

The performances of the gain mirrors were characterized in a V-shaped VECSEL cavity (Fig. 6). The gain chips were optically pumped with 808-nm fibre-coupled diode lasers at a copper mount temperature of 15 °C. The calculated pump spot diameters on the gain mirror surfaces, not taking into account the pump angle, were 124 and 180 μm for $S1$ and $S2$, respectively. Therefore, the pump spot area used in $S2$ characterization was about twice the area used in $S1$ characterization. The pump beam was set at a 40° angle for $S1$ and at a 35° angle for $S2$. The $S1$ mount was cooled by a water cooling circuit and $S2$ was cooled by a thermoelectric cooler, which in turn was water cooled. For independent characterization the output wavelengths were separated with the aid of a dichroic beam splitter. The temporal behaviours of the separated beams were studied by measuring the intensities with a 1-GHz silicon detector. The output powers of the beams were measured with two calibrated thermopile sensors. The output spectra of the lasers were studied without the dichroic filter.

4. Results and discussions

The laser using the $S1$ gain mirror emitted light at wavelengths of $\lambda_{S,S1} = 982$ nm and $\lambda_{L,S1} = 1042$ nm (see Fig. 7), while the laser based on $S2$ mirror emitted light at $\lambda_{S,S2} = 966$ nm and $\lambda_{L,S2} = 1047$ nm (see Fig. 8). Consequently, the wavelength separation, $\Delta\lambda$, was 60 nm for $S1$ and 81 nm for $S2$.

$S1$ generated maximum continuous-wave (cw) optical power of 0.14 W at $\lambda_{S,S1}$ and 0.115 W at $\lambda_{L,S1}$ (Fig. 9) with maximum slope efficiencies of 10 and 8%, respectively. The lasing thresholds were reached at
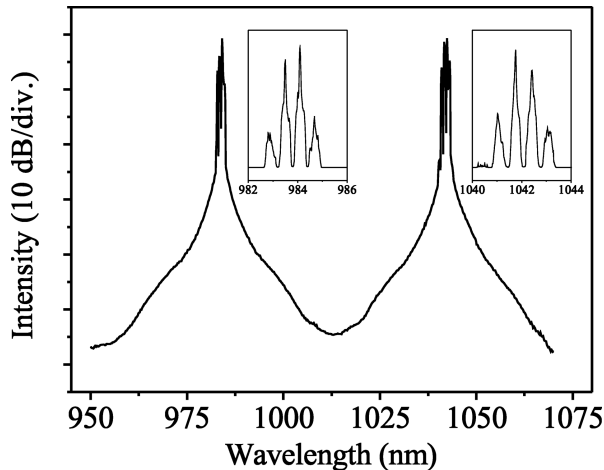
Fig. 7. Output spectrum of the VECSEL using $S1$ gain mirror. The insets show spectra on a magnified scale close to the emission peaks.
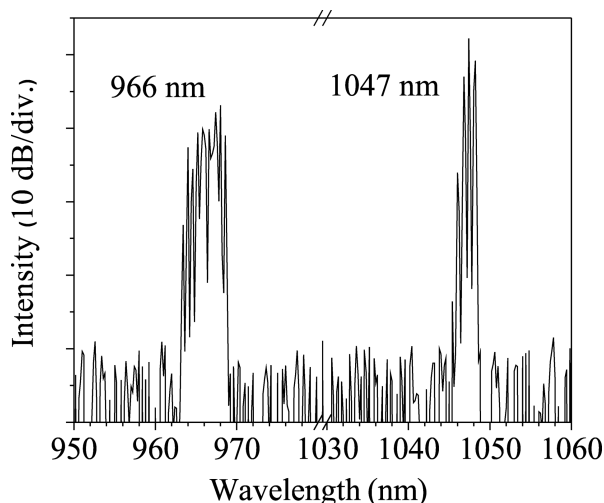

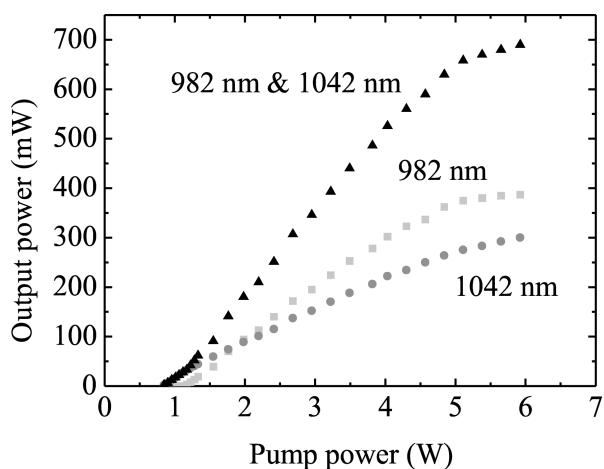Fig. 8. Output spectrum of the VECSEL using the gain mirror $S2$.

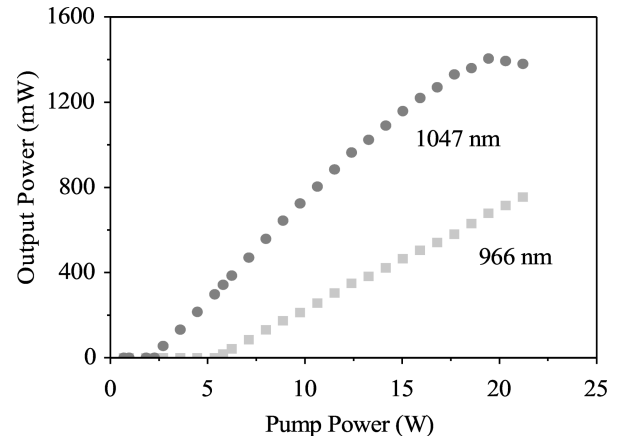Fig. 9. Light output graph of the VECSEL using $S1$ gain mirror.

Fig. 10. Light output graph of the VECSEL using $S2$ gain mirror.

pump powers of 1.15 W for $\lambda_{S,S1}$ and 0.85 W for $\lambda_{L,S1}$. The laser output remained cw up to a pump power of 2.4 W. Beyond this pump power, both wavelengths showed strong in-phase self pulsation. The maximum combined output power of both wavelengths in this self-pulsating mode was about 700 mW at a pump power of 6 W, corresponding to a $\lambda_{S,S1}$ output power of about 390 mW and a $\lambda_{L,S1}$ power of about 300 mW. In both x and y directions, the beam propagation factor was $M^2 = 1.04$, which indicates excellent beam quality.

The laser using the $S2$ gain mirror generated maximum cw optical power of 0.75 W at $\lambda_{S,S2}$ at the pump power of 21.2 W and 1.4 W at $\lambda_{L,S2}$ at the pump power of 19.4 W (Fig. 10). The lasing thresholds were reached at the pump powers of 5.4 and 2.3 W for $\lambda_{S,S2}$ and $\lambda_{L,S2}$, respectively. M^2 was 1.38 in the x direction and 1.51 in the y direction. Like the VECSEL using the gain mirror $S1$, both wavelengths showed self-pulsating behaviour at output powers exceeding 300 mW. The maximum output powers in the self-pulsating mode was about 750 mW for $\lambda_{S,S2}$ and 1400 mW for $\lambda_{L,S2}$. The combined output power reached its maximum of about 2100 mW at a pump power of 21 W. The maximum slope efficiencies for $\lambda_{S,S2}$ and $\lambda_{L,S2}$ were approximately 5 and 10%, respectively.

The VECSEL using the $S2$ gain mirror generated a higher maximum optical output power at each wavelength as compared to the VECSEL using the $S1$ gain mirror. This difference is not entirely explained by the difference in the pump spot size alone, which was about twice as large for the VECSEL using the gain mirror design $S2$ than the VECSEL using the gain mirror design $S1$. Therefore, it seems that $S2$ is a more suitable design for high-power operation. This may be due to the larger number of QWs for both wavelengths in $S2$. The wavelength separation is greater for the VECSEL using the $S2$ gain mirror than for the VECSEL using the

*S*1 gain mirror. This is because the separated feedback of λ_L and λ_S allows the $\Delta\lambda$ to exceed the AlAs/GaAs DBR stop-band width.

The gain equalization was more successful in *S*1 than in *S*2. In *S*2, λ_L exhibited lower threshold and higher slope efficiency than λ_S, despite the higher thermal impedance between the λ_L gain region and the diamond heat spreader. The higher thermal impedance, however, may be the reason why λ_L exhibits thermal roll-over at lower pump powers than λ_S. The higher slope efficiency of λ_L in the VECSEL using the *S*1 gain mirror can be attributed to the depth of the λ_L QWs, which, being deeper than the λ_S QWs, have higher carrier capture efficiency [12]. The capture efficiency may also be the cause of the thermal roll-over behaviour observed in the same VECSEL – in this VECSEL, where the thermal impedance of both wavelength's gain regions are similar, λ_S rolls over at a lower pump intensity than λ_L.

To improve the designs, the gain equalization of *S*2 can be enhanced by reducing the number of λ_L QWs and its RPG structure thickness. At the same time, the number of λ_S QWs, together with the λ_S RPG structure thickness, should be increased in order to use the pump light effectively. The wavelength separation achieved with *S*1 can be increased by the use of multi-stop-band DBRs [16]. To suppress self-pulsating behaviour, λ_S should be better isolated from the λ_L gain medium. The power levels achieved are high enough to enable efficient intra-cavity frequency mixing.

5. Conclusions

We have designed and fabricated two different vertical-cavity surface-emitting laser (VECSEL) gain mirrors that are capable of providing gain simultaneously at two well-separated wavelengths. The first design, *S*1, had one gain region and the second design, *S*2, had two gain regions, one for each wavelength, separated by an optical long-wave pass filter. The VECSEL using the *S*1 gain mirror design generated a maximum optical power of 0.39 W (140 mW in continuous wave mode) at 982 nm and 0.3 W (115 mW) at 1042 nm, whereas the VECSEL using the *S*2 gain mirror design generated 0.75 W (300 mW) at 966 nm and 1.38 W (300 mW) at 1047 nm. Both lasers exhibited self-pulsation at high output powers. *S*1 sets higher requirements on growth precision, but the VECSEL using this gain mirror design exhibited better equalized output power between the wavelengths. In addition to higher output power, the VECSEL using the *S*2 gain mirror design exhibited

a larger separation between the operation wavelengths. Based on our experiments, we believe dual-wavelength VECSELs are a suitable route for demonstrating a compact solution for dual-wavelength emission and intra-cavity difference frequency generation.

References

[1] W. Chen, J. Cousin, E. Poullet, J. Burie, D. Boucher, X. Gao, M.W. Sigrist, and F.K. Tittel, Continuous-wave mid-infrared laser sources based on difference frequency generation, Comptes Rendus Physique **8**(10), 1129–1150 (2007).

[2] C. Wang, Y. Chuang, and C. Pan, Two-wavelength interferometer based on a two-color laser-diode array and the second-order correlation technique, Opt. Lett. **20**(9), 1071–1073 (1995).

[3] P. Pellandini, R.P. Stanley, R. Houdre, U. Oesterle, M. Ilegems, and C. Weisbuch, Dual-wavelength laser emission from a coupled semiconductor microcavity, Appl. Phys. Lett. **71**(7), 864–866 (1997).

[4] C.-F. Lin, M.-J. Chen, and B.-L. Lee, Wide-range tunable dual-wavelength semiconductor laser using asymmetric dual quantum wells, IEEE Photon. Technol. Lett. **10**(9), 1208–1210 (1998).

[5] C.-C. Huang, C.-H. Cheng, Y.-S. Su, and C.-F. Lin, 174-nm mode spacing in dual-wavelength semiconductor laser using nonidentical InGaAsP quantum wells, IEEE Photon. Technol. Lett. **16**(2), 371–373 (2004).

[6] N. Basov, O. Bogdankevich, and A. Grasyuk, 9B4–semiconductor lasers with radiating mirrors, IEEE J. Quantum Electron. **2**(9), 594–597 (1966).

[7] M. Kuznetsov, F. Hakimi, R. Sprague, and A. Mooradian, High-power (>0.5-W CW) diode-pumped vertical-external-cavity surface-emitting semiconductor lasers with circular TEM$_{00}$ beams, IEEE Photon. Technol. Lett. **9**(8), 1063–1065 (1997).

[8] A. Tropper and S. Hoogland, Extended cavity surface-emitting semiconductor lasers, Prog. Quantum Electron. **30**(1), 1–43 (2006).

[9] S. Giet, A.J. Kemp, D. Burns, S. Calvez, M.D. Dawson, S. Suomalainen, A. Harkonen, M. Guina, O. Okhotnikov, and M. Pessa, Comparison of thermal management techniques for semiconductor disk lasers, in: *Solid State Lasers XVII: Technology and Devices*, eds. W.A. Clarkson, N. Hodgson, and R.K. Shori, Proc. SPIE **6871**, 687115-10 (2008).

[10] W.J. Alford, T.D. Raymond, and A.A. Allerman, High power and good beam quality at 980 nm from a vertical

external-cavity surface-emitting laser, J. Opt. Soc. Am. B **19**(4), 663–666 (2002).

[11] J. Hopkins, A.J. Maclean, D. Burns, E. Riis, N. Schulz, M. Rattunde, C. Manz, K. Köhler, and J. Wagner, Tunable, single-frequency, diode-pumped 2.3-μm VECSEL, Opt. Express **15**(13), 8212–8217 (2007).

[12] T. Leinonen, Y. Morozov, A. Harkonen, and M. Pessa, Vertical external-cavity surface-emitting laser for dualwavelength generation, IEEE Photon. Technol. Lett. **17**(12), 2508–2510 (2005).

[13] Y. Morozov, T. Leinonen, A. Harkonen, and M. Pessa, Simultaneous dual-wavelength emission from vertical external-cavity surface-emitting laser: A numerical

modeling, IEEE J. Quantum Electron. **42**(9–10), 1055–1061 (2006).

[14] T. Leinonen, S. Ranta, A. Laakso, Y. Morozov, M. Saarinen, and M. Pessa, Dual-wavelength generation by vertical external cavity surface-emitting laser, Opt. Express **15**(20), 13451–13456 (2007).

[15] Z.L. Liau, Semiconductor wafer bonding via liquid capillarity, Appl. Phys. Lett. **77**(5), 651–653 (2000).

[16] S. Calvez, D. Bums, and M.D. Dawson, Optimization of an optically pumped 1.3-μm GaInNAs verticalcavity surface-emitting laser, IEEE Photon. Technol. Lett. **14**(2), 131–133 (2002).

VIENALAIKIS DVIEJŲ BANGŲ GENERAVIMAS IŠ PUSLAIDININKINIŲ VERTIKALIAI SPINDULIUOJANČIO PAVIRŠIAUS LAZERIŲ SU IŠORINIU REZONATORIUMI

S. Ranta [a], T. Leinonen [a], A. Härkönen [a], A. Laakso [a], Y. Morozov [b], M. Pessa [a]

[a] _Tamperės technologijos universiteto Optoelektronikos mokslinių tyrimų centras, Tamperė, Suomija_
[b] _Rusijos MA Radijo inžinerijos ir elektronikos instituto Saratovo skyrius, Saratovas, Rusija_

Santrauka

Pademonstruotas dviejų bangų generavimas iš optiškai kaupinamo vertikaliai spinduliuojančio paviršiaus lazerio su išoriniu rezonatoriumi (angl. tokio lazerio trumpinys yra VECSEL), naudojant dviejų skirtingų konstrukcijų stiprinančiuosius veidrodžius. Pirmoji stiprinančiojo veidrodžio konstrukcija ($S1$) leido generuoti 0,39 W galios $\lambda_S = 984$ nm bangos ilgio spinduliuotę ir 0,30 W galios $\lambda_L = 1042$ nm spinduliuotę. VECSEL lazeris su antrąja stiprinančiojo veidrodžio konstrukcija ($S2$) generavo maksimalią 0,75 W

galios spinduliuotę, kurios bangos ilgis $\lambda_S = 966$ nm, ir 1,38 W galios spinduliuotę, kurios bangos ilgis $\lambda_L = 1047$ nm. VECSEL lazeriai su abiejų konstrukcijų stiprinančiaisiais veidrodžiais išsiskyrė savipulsacija esant didelių išvadinių galių režimui. Lazeryje su $S1$ konstrukcijos stiprinančiuoju veidrodžiu savipulsacijos prasidėdavo bangos λ_S galiai viršijus 140 mW, o bangos λ_L – viršijus 115 mW. Lazeryje su $S2$ konstrukcijos stiprinančiuoju veidrodžiu savipulsacijos atsiradimo slenkstis esant atitinkamiems abiejų bangų ilgiams buvo 300 mW.